PAPER

Check for updates

Self-healing amino acid-bearing acrylamides/*n*-butyl acrylate copolymers *via* multiple noncovalent bonds†

Ryo Kudo,[a] Sadaki Samitsu [ID] [b] and Hideharu Mori [ID] *[a]

Four amino acid-bearing acrylamides, *N*-acryloyl-L-threonine (AThrOH), *N*-acryloyl-L-glutamic acid (AGluOH), *N*-acryloyl-L-phenylalanine (APheOH), and *N*-acryloyl-L, L-diphenylalanine (APhePheOH), were selected for copolymerization with *n*-butyl acrylate (*n*BA) to develop amino acid–based self-healable copolymers. A series of copolymers comprising amino acid-bearing acrylamides and *n*BA with tunable comonomer compositions and molecular weights were synthesized by free radical and reversible addition–fragmentation chain-transfer copolymerization. Self-healing and mechanical properties originated from the noncovalent bonds between the carboxyl, hydroxyl, and amide groups, and $\pi-\pi$ stacking interactions among the amino acid residues in the side chains were evaluated. Among these copolymers, P(*n*BA-*co*-AGluOH) with suitable comonomer compositions and molecular weights (*n*BA : AGluOH = 82 : 18, M_n = 18 300, M_w/M_n = 2.58) exhibited good mechanical properties (modulus of toughness = 17.3 MJ m^{-3}) and self-healing under ambient conditions. The multiple noncovalent bonds of P(*n*BA-*co*-AGluOH)s were also efficient in improving the optical properties with an enhanced refractive index and good transparency.

Introduction

Self-healing materials that can heal damages have emerged as promising materials for sustainable societies and numerous industrial applications.[1–4] In addition to extrinsic self-healing materials utilizing a healing agent,[5,6] a variety of intrinsic self-healing materials have been developed, which relied mainly on covalent dynamic bonds (*e.g.*, urea bond,[7,8] trithiocarbonate unit,[9] disulfide bond,[10,11] Diels–Alder reaction,[12–14] and transesterification[15,16]) and noncovalent reversible interactions (*e.g.*, hydrogen bonds,[17–19] ionic interactions,[20] $\pi-\pi$ interactions,[21–23] and metal–ligand coordination[24–26]). The incorporation of such self-healing units into polymeric materials with sophisticated designs is crucial for achieving desirable self-healing properties, mechanical properties, and targeted functions. For instance, various supramolecular hydrogels showing essential functions, *e.g.*, self-healing, stimuli-responsive, biocompatible, antibacterial, antioxidant, and tissue-adhesive functions, have been developed for biomedical and clinical applications.[27,28] The capability to utilize conventional and industrially applicable processes that can be extended to future large-scale production is desirable.

Self-healing can be found in living organisms, which originated from physical and chemical changes in response to environmental change.[4] Peptides and amino acids, which are constitution units for proteins, have attracted considerable attention as bio-mimics and critical units for self-healing polymers and gels, demonstrating various advantages, such as nontoxicity, biodegradability, and hydrophilicity.[29] These systems can be governed by abundant units, such as hydrogen bonds, electrostatic and hydrophobic interactions, leading to supramolecular self-assembly (*e.g.*, β-sheets). Because amino acids with the general form RCH(NH$_2$)COOH have an amino group, a carboxyl group, and other functional groups depending on the structure of the R group, their derivatives have been intensively employed as constituent units for various self-healing materials. For example, various self-healable hydrogels and shape memory polymer networks have been developed utilizing amino acid derivatives and polymers, such as chitosan/acryloyl-phenylalanine,[30] poly(aspartic acid),[31] poly(γ-glutamic acid),[32,33] poly(L-glutamic acid)/ureido-pyrimidinone,[34] acryloyl-6-aminocaproic acid,[35] *N*-acryloyl glycinamide,[36] *N*-acryloyl glycinamide/*N*-acryloyl serine methyl ester[37] and *N*-acryloyl alanine.[38] These hydrogels and polymer networks mainly relied on chemical crosslinking, occasionally combined with physical crosslinking originating from amino acid-derived hydrogen bonds. Interestingly, *N*-acryloyl glycinamide was found to form supramolecular hydrogels directly *via* physical crosslinking

[a]Department of Organic Material Science, Graduate School of Organic Materials Science, Yamagata University, 4-3-16, Jonan, Yonezawa City, Yamagata Prefecture 992-8510, Japan. E-mail: h.mori@yz.yamagata-u.ac.jp

[b]National Institute for Materials Science, 1-2-1, Sengen, Tsukuba, 305-0047, Japan

† Electronic supplementary information (ESI) available. See DOI: https://doi.org/10.1039/d4ra00800f

owing to dual amide motifs.[36] In addition, side-chain type (*e.g.*, triblock and multiblock copolymers with *N*-acryloyl-L-phenylalanine[39]) and main-chain type (*e.g.*, multiblock copolymers with oligopeptides,[40] polydimethylsiloxane with L-phenylalanine unit[41]) polymers have been explored, which have amino acid/peptide units that act as physical crosslinking motifs in the side chain and main chain. Furthermore, low-molecular-weight amino acid/peptide derivatives (*e.g.*, phenylalanine,[42] nucleotripeptides[43]) have been employed as self-healing gelators.[44]

n-Butyl acrylate (*n*BA) is one of the most widely utilized monomers for producing rubbers and elastomers owing to the low glass transition temperature (T_g) of the resulting poly(*n*BA). Hence, it has been widely employed as a flexible component for self-healing elastomers, gels, and networks. For instance, carboxylic acid-containing monomers (*e.g.*, acrylic acid[45,46] and acrylic acid/vinylimidazole[47]) and hydroxyl group-containing monomers (*e.g.*, dopamine acrylamide[48,49] and *N*-(hydroxymethyl)acrylamide[50]) have been copolymerized with *n*BA to form self-healable polymers. Their healing and physical properties were mainly governed by noncovalent interactions (*e.g.*, hydrogen bonds, ionic interactions, and metal coordination) from the functional units and the flexibility from *n*BA units. The hydrophobic association of *n*-butyl groups of *n*BA units in copolymer chains has been occasionally utilized to form a physical hydrogel, depending on the environment (*e.g.*, in aqueous solution).[51] A variety of functional monomers, such as (2-acetoacetoxy)ethyl methacrylate,[52] epoxy- and urea-containing methacrylates,[53] 1-vinylimidazole,[54] 2,2,2-trifluoroethyl methacrylate,[55] have also been utilized for *n*BA-based self-healable polymeric materials. Other attractive features of *n*BA-containing copolymers include excellent biocompatibility, stability, and good adhesion; therefore, *n*BA has been utilized in biocompatible gels,[56–58] networks,[59,60] and copolymers.[61,62]

Here, we described a straightforward and efficient approach for developing self-healing copolymers by incorporating amino acid units into *n*BA-based elastomers *via* free-radical copolymerization (Fig. 1). Four acrylamides bearing different amino acids, *N*-acryloyl-L-threonine (AThrOH),[63,64] *N*-acryloyl-L-glutamic acid (AGluOH),[65,66] *N*-acryloyl-L-phenylalanine (APheOH)[67] and *N*-acryloyl-L,L-diphenylalanine (APhePheOH)[68] were selected attempting to tune intra- and intermolecular noncovalent interactions (*e.g.*, hydrogen bonds, electrostatic interactions, and π−π stacking) and their flexibilities. AThrOH has a hydroxyl group and a carboxyl group, AGluOH has two carboxyl groups, and APheOH has a carboxyl group and a phenyl group, in addition to an amide group in each monomer unit. APhePheOH contains two amide groups, two phenyl group, and one carboxyl groups. The core of our strategy is the selection of suitable amino acid-bearing acrylamides, which can act as self-healing sites *via* noncovalent interactions, combined with *n*BA, which can contribute to tuning the flexibility. By exploiting this unique combination of naturally originating hydrophilic building blocks derived from amino acids and nonionic *n*BA as a hydrophobic unit, we demonstrated tunable physical, optical, and self-healing properties. The unique intrinsic features of the copolymers, *e.g.*, good transparency, tunable refractive indexes and softness, can be applied for ophthalmic optics in future applications. The introduction of chirality originated from amino acid units is another attractive feature of the copolymers, which can extend to advanced materials, such as aggregation-induced circular dichroism and circularly polarized luminescence materials.[69–71]

Results and discussion

Copolymer synthesis

Amino acid–based random copolymers were initially synthesized by free radical copolymerization of *n*BA and acrylamides bearing different amino acids (AThrOH, AGluOH, APheOH, and APhePheOH) with AIBN under the appropriate conditions (Table S1 and Scheme S1†). The chemical structure and comonomer composition were verified *via* proton nuclear magnetic resonance (^1H NMR) spectroscopy (Fig. S1–S6†), and the molecular weight and dispersity were verified by size exclusion chromatography (SEC) measurement of the methylated sample (Fig. S7–S10†). For instance, the copolymerization of *n*BA and AThrOH was performed with various comonomer feed ratios $[nBA]_0/[AThrOH]_0 = 50:150, 100:100, 150:50, 175:25$ at a constant monomer-to-initiator ratio $[nBA + AThrOH]_0/[AIBN]_0 = 200:1$ in ethanol at 60 °C for 24 h. Targeted P(*n*BA-*co*-AThrOH)s with various tunable comonomer compositions (AThrOH content = 10–65 mol%, as determined by ^1H NMR, Fig. S4†) with similar molecular weights ($M_{n,SEC}$ = 18 400–30 800, M_w/M_n = 2.57–3.17, Fig. S8†) were obtained in good polymer yields of 81–90%, after the reprecipitation from hexane. Similarly, P(*n*BA-*co*-AGluOH)s with tunable AGluOH contents (8–49 mol%) with reasonable molecular weights and polymer yields ($M_{n,SEC}$ = 15 100–29 400, M_w/M_n = 2.06–2.60, yield = 74–98%), as illustrated in Fig. S7.† The *n*BA content in P(*n*BA-*co*-AGluOH)s (51–92%) is higher than the feed ratio ($[nBA]_0/[AGluOH]_0 = 50:150–175:25$), indicating a preferable insertion of *n*BA during the copolymerization. For the synthesis of P(*n*BA-*co*-APheOH) and P(*n*BA-*co*-APhePheOH), the copolymerization was conducted at [AIBN]/[*n*BA]/[amino acid-bearing monomer] at 1/150/50 at 60 °C in DMF, affording the copolymers with
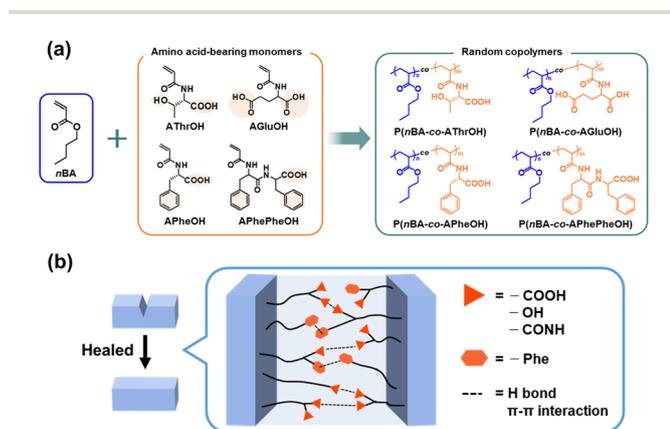

Fig. 1 (a) Synthesis and (b) postulated healing process of amino acid–based random copolymers.

targeted molecular weights and comonomer compositions ($M_{n,SEC}$ = 27 200–46 400, M_w/M_n = 2.51–2.83, nBA content = 86–88 mol%, and yield = 68–73%).

All copolymers bearing different amino acids (AThrOH, AGluOH, APheOH, and APhePheOH) were dissolved in DMF and DMSO (Tables S2–S4†). Owing to the amphiphilic nature, these copolymers were soluble in specific solvents (e.g., THF, chloroform, methanol, and basic water), dependent on the nature of the amino acid units and composition. For instance, P(nBA-co-AGluOH) with 82 mol% nBA content was soluble in THF an methanol, while insoluble in neutral water. These copolymers exhibited no detectable swelling and degradation (Fig. S11†), owing to the linear (Fig. 1) chain structures consisted of carbon–carbon backbone without cross-linking/ network formation. Note that the threonine- and glutamic acid-based homopolymers (PAThrOH[63] and PAGluOH[65]) were soluble in water, independent of the pH value. In contrast, the phenylalanine- and diphenylalanine-based homopolymers (PAPheOH[67] and PAPhePheOH[68]) were only soluble in basic water (pH > 12) but insoluble in acidic and neutral water, owing to pH-dependent degree of the ionization.

Fig. 2 shows attenuated total reflection Fourier transform infrared (ATR FT-IR) spectra of the copolymers with different amino acid units. Characteristic absorption bands due to the carbonyl (1730 cm^{-1}) and C–H stretching vibrations (2775–3020 cm^{-1}) are clearly observed for all copolymers. ATR FT-IR spectra of the copolymers reveal characteristic broad absorption at 3100–3420 cm^{-1} (Fig. 2b), corresponding to an amide hydrogen bonded N–H.[72,73] Among four copolymers, P(nBA-co-AGluOH) and P(nBA-co-AGluOH) exhibit remarkable broad absorbance in the region below 3400 cm^{-1}, suggesting the presence of multiple hydrogen bonds. In all copolymers, characteristic absorption of the amide I is detected at approximately 1650 cm^{-1}, which reflects the secondary structure.[40] In addition to the clear peak attributed to ester carbonyl band at 1730 cm^{-1}, a broad shoulder absorbance is detected at approximately 1700 cm^{-1}, depending on the copolymer. Similar tendency was

observed for ATR FT-IR spectra of the homopolymers (PAThrOH, PAGluOH, PAPheOH, and PAPhePheOH, Fig. S12†). These results suggest the present of different intramolecular (or intermolecular) interactions, originated from the nature of amino acids, which may affect the thermal, mechanical, and self-healing properties of the copolymers.

Thermal and mechanical properties

The thermal properties of the P(nBA-co-AGluOH)s with different nBA contents (52–92 mol%) were investigated by thermogravimetric analysis (TGA) and differential scanning calorimetry (DSC). As illustrated in Fig. 3a, all P(nBA-co-AGluOH)s exhibited high thermal stability (5% mass loss temperature T_{d5}> 250 °C under nitrogen conditions), and the T_{d5} value increased with increasing nBA content, e.g., T_{d5} = 280 °C for the copolymer with highest nBA content (92 mol%). The glass transition temperature (T_g) value of P(nBA-co-AGluOH)s decreased from 55.1 °C to −20.5 °C when the nBA content increased from 51 to 92 mol% (Fig. 3b). The same trends were seen for P(nBA-co-AThrOH)s, which revealed an increase in the T_{d5} value from 187 to 213 °C and a decrease in the T_g value from 134.1 to −37.8 °C with increasing nBA content from 35 to 90 mol% (Fig. S13 and Table S5†).

The dog bone-shaped species were prepared from P(nBA-co-AGluOH)s having different comonomer compositions utilizing a Teflon mold at 100–120 °C by hot-press for 1–3 min (Table S6†), followed by cooling at an ambient condition, for tensile test. P(nBA-co-AGluOH) with 92 mol% nBA was viscous with fluid properties, making it difficult to maintain the molded shape (Fig. 3c). In contrast, rubbery samples were obtained from P(nBA-co-AGluOH) with 82 mol% nBA content, which has substantial mechanical properties and flexibility and was bent and twisted without breaking (Fig. 3d). A further decrease in the nBA content (e.g., less than 70 mol%) led to the formation of glassy and fragile samples broken by shearing a small amount
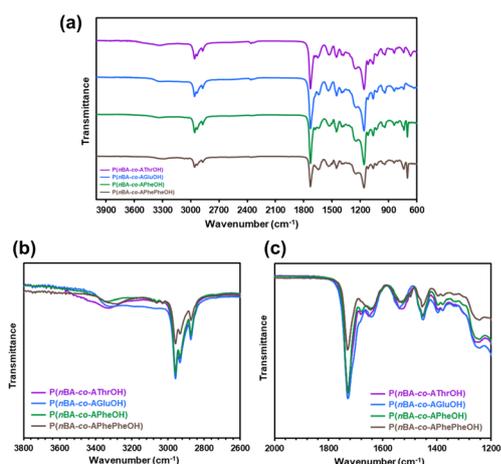

Fig. 2 (a) ATR FT-IR spectra of amino acid-based copolymers (nBA content = approximately 80 mol%) and magnification in the region of (b) N–H band and (c) carbonyl band.
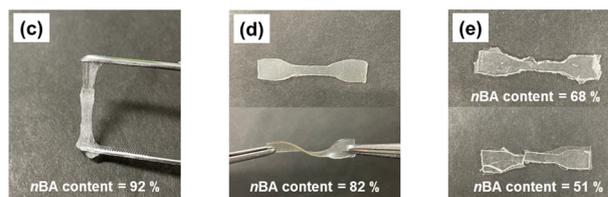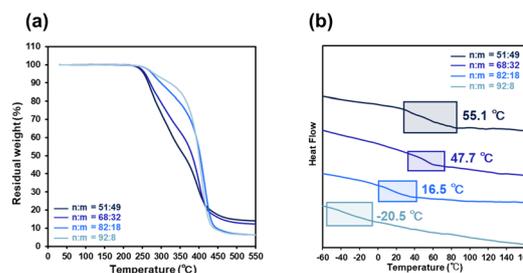

Fig. 3 (a) TGA traces (b) DSC traces of P(nBA-co-AGluOH)s (nBA content = 51–92 mol%) and (c–e) appearance of P(nBA-co-AGluOH) (nBA content = 51–92 mol%).

of stress (Fig. 3e), implying that a higher AGluOH content led to higher noncovalent interactions and lower nBA, which caused the copolymer to behave as a brittle plastic. Hence, as expected, the comonomer composition significantly influenced the thermal and mechanical properties of P(nBA-co-AGluOH)s. This implied that the noncovalent interactions of the amino acid units (*e.g.*, hydrogen bonds and electrostatic interactions derived from the AGluOH unit in this case) were crucial factors in manipulating the intermolecular interactions between the copolymer chains.

The thermal and physical properties of the four copolymers bearing different amino acids (AThrOH, AGluOH, APheOH, and APhePheOH) were compared, and the results are summarized in Table 1. Copolymers with similar molecular weights and comonomer compositions ($M_{n,SEC} = 18\,300\text{–}46\,400$, and nBA content = 80–88 mol%) were selected to clarify the effects of noncovalent interactions derived from the amino acid unit. When the aromatic amino acid units were incorporated into the side chains, thermally stable copolymers were obtained ($T_{d5} = 309$ and 288 °C for the copolymers with APheOH and APhePheOH), which were higher than those with aliphatic amino acid units ($T_{d5} = 200$ and 270 °C for the copolymers with AThrOH and AGluOH), as illustrated in Fig. 4a. The T_g values of the copolymers with AThrOH, AGluOH, and APhePheOH units ranged between 27.3–16.5 °C. In contrast, a lower T_g value (-5.1 °C) was seen for P(nBA-co-APheOH), as depicted in Fig. 4b. Slightly lower T_g (16.5 °C) of P(nBA-co-AGluOH), compared to those of P(nBA-co-AThrOH) and P(nBA-co-APhePheOH) (27.3 and 21.5 °C) may be attributed to the presence of flexible alkyl chain in AGluOH unit. These copolymers possess easy processability that are moldable at a certain temperature, which can be tuned by selecting the nature of the amino acid units and their composition.

The mechanical properties of four amino acid-based copolymers were evaluated by tensile stress–strain tests at room temperature (approximately 23–26 °C, Fig. 4c, d and Table 1). Young's moduli of the copolymers with AThrOH, AGluOH, and APhePheOH units ranged between 97–148 MPa. In contrast, a lower value (5.1 MPa) was observed for P(nBA-co-APheOH), demonstrating the highest strain of more than 900% without fracture. P(nBA-co-AThrOH) exhibited the highest maximum strength (11.0 MPa), whereas failure owing to brittleness was
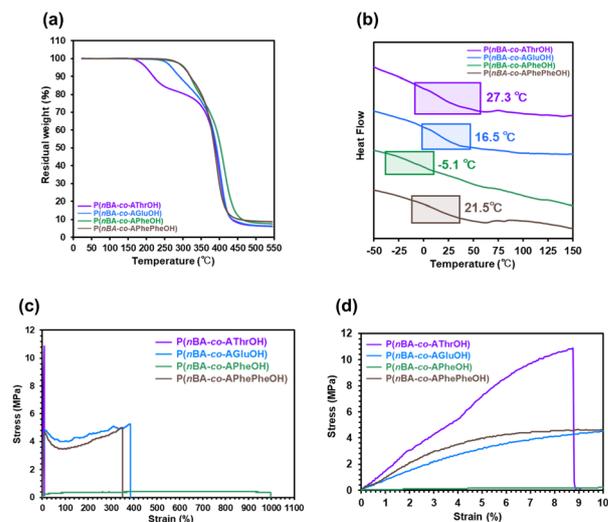

Fig. 4 (a) TGA traces (b) DSC traces of amino acid-based copolymers (nBA content = approximately 80 mol%) and (c and d) stress–strain curves of the random copolymers (nBA content = approximately 80 mol%) in (c) 0–1100% strain and (d) 0–10% strain.

detected when the rupture strain reached 8.8%. Among the four copolymers, P(nBA-co-AGluOH) exhibited a good balance of moderate Young's modulus (97 MPa) and the highest modulus of toughness (17.3 MJ m^{-3}) and was therefore utilized for the self-healing test.

Self-healing properties

Fig. 5a illustrates a preliminary demonstration of the self-healing capability of P(nBA-co-AGluOH) with 82% nBA content. A dog bone-shaped specimen prepared by hot press at 100 °C for 1 min can pull without breaking and then return to the original shape, implying stretchable and good mechanical properties. The specimens were cut into two pieces and manually pressed. The fractured surfaces of P(nBA-co-AGluOH) were rejoined after being pressed together with the cut samples for approximately 30 s under ambient conditions (approximately 25 °C). Similarly, the fractured surfaces of P(nBA-co-AThrOH) were rejoined by pressing at 40 °C for 30 min

Table 1 Characteristics of amino acid–based copolymers (nBA content = approximately 80 mol%)

Copolymer	$M_n{}^a$ (SEC)	$n:m^b$	$T_{d5}{}^c$ (°C)	$T_g{}^d$ (°C)	Young's modulus^e (MPa)	Maximum strength (MPa)	Maximum strain (%)	Modulus of toughness^f (MJ m^{-3})
P(nBA-co-AThrOH)	18 400	80 : 20	200	27.3	148	11.0	8.8	0.54
P(nBA-co-AGluOH)	18 300	82 : 18	270	16.5	97	5.2	385	17.30
P(nBA-co-APheOH)	46 400	88 : 12	309	−5.1	5.1	0.40	997	3.95
P(nBA-co-APhePheOH)	27 200	86 : 14	288	21.5	109	5.0	350	14.08

^{a} This was evaluated by SEC. ^{b} ^{1}H NMR (Table S1). ^{c} 5 wt% loss temperature. ^{d} Glass transition temperature. ^{e} Calculated from stress at slight strain (<5%). ^{f} Estimated by area under stress–strain until fracture point.
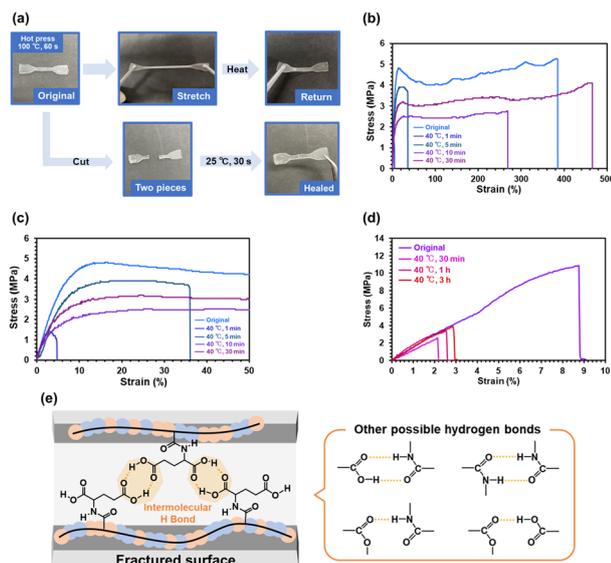
Fig. 5 (a) Photos of original, stretched, and recovered P(nBA-co-AGluOH) sample and preliminary healing test. Stress–strain curves of (b and c) P(nBA-co-AGluOH) after healing in (b) 0–500% strain and (c) 0–50% strain, and (d) P(nBA-co-AThrOH) after healing and (e) schematics of healing process of P(nBA-co-AGluOH).

(Fig. S14†), suggesting that the copolymer with AThrOH demonstrated self-healable property. Still, the self-healable property was less than that with AGluOH. In contrast, P(nBA-co-APheOH) and P(nBA-co-APhePheOH) having aromatic amino acids exhibited no healing capability, even if the healing temperature increased up to 50–60 °C (Fig. S15 and Table S7†), which may be due to the interference of the hydrogen bonds by bulky aromatic units in APheOH and APhePheOH. Further studies were required to determine optimal comonomer compositions and sequences of these aromatic amino acid–based copolymers. Nevertheless, these results suggest that a suitable selection of the amino acid unit and its composition with nBA units are essential for achieving reasonable self-healing and mechanical properties of the nBA/amino acid–based copolymers by tuning suitable noncovalent interactions.

The self-healing efficiencies of P(nBA-co-AGluOH) and P(nBA-co-AThrOH) were evaluated by comparing maximal strength of the pristine specimen and healed ones treated at 40 °C for different compression time (Fig. 5 and Table S8†). Both copolymer samples demonstrated improved self-healing capabilities with increasing compression time. Notably, P(nBA-co-AGluOH) recovered 90% of the maximum strength of the pristine sample after 30 min compression (Fig. 5b and c). In contrast, P(nBA-co-AThrOH) recovered approximately 10%, even after 3 h (Fig. 5d). These results suggest that intermolecular hydrogen bonds between two carboxylic acids in the AGluOH unit, in addition to carboxylic acid/amide and amide/amide hydrogen bonds, are essential for achieving reasonable self-healing ability (Fig. 5e). Obviously, self-healing properties are affected by molecular mobility of the copolymer chain. Therefore, each copolymer having different T_g values possess suitable healing temperature. In this study, the self-healing behaviors of the copolymers

having different animo acid units were compared at 40 °C, which are higher than those of T_g values of the copolymers (−5.1–27.3 °C). Further studies on the amino acid–based copolymers, such as the influence on the healing temperature on the healing properties and temperature-dependent rheological behavior, will be reported separately.

Effect of molecular weight

P(nBA-co-AGluOH)s with different molecular weights and approximately the same comonomer composition (nBA/AGluOH molar ratio = approximately 8/2) were synthesized to evaluate the effect of the molecular weight on the mechanical and self-healing properties (Table S9†). RAFT copolymerization of nBA and AGluOH utilizing a trithiocarbonate-type chain transfer agent (CTA) at different monomer-to-CTA ratios ([nBA + AGluOH]/[CTA] = 100–400) at a constant CTA-to-initiator and a comonomer feed ratio ([CTA]$_0$/[AIBN]$_0$ = 2/1 and [nBA]/[AGluOH] = 3/1) produced P(nBA-co-AGluOH)s with adjustable molecular weights (M_n = 9500–15 900). When RAFT copolymerization was conducted at [nBA]/[AGluOH]/[CTA]/[AIBN] = 150/50/2/1–300/100/2/1, P(nBA-co-AGluOH)s having relatively low disparities (M_w/M_n = 1.25–1.36) were obtained, while further increase in the monomer-to-CTA ratio led to the broadening disparity (M_w/M_n = 1.79), as depicted in Fig. 6a. As comparisons, P(nBA-co-AGluOH)s having higher molecular weights (M_n = 18 300–21 500, M_w/M_n = 2.58–2.73) with (nBA/AGluOH = approximately 8/2 molar ratio) were prepared by free radical copolymerization at different [nBA]/[AGluOH]/[AIBN] ratios (150/50/1 and 300/100/1). P(nBA-co-AGluOH) samples of different molecular weights were utilized to evaluate their thermal and mechanical properties (Table S9† and Fig. 6).
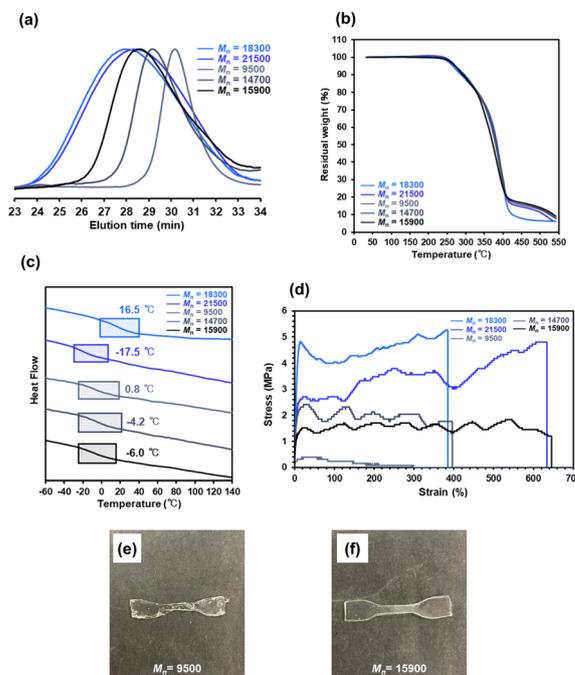

Fig. 6 (a) SEC, (b) TGA, and (c) DSC traces, and (d) stress–strain curves of P(nBA-co-AGluOH)s (M_n = 9500–21 500) and (e and f) appearance of P(nBA-co-AGluOH)s (M_n = 9500, 15 900).

TGA results revealed that P(nBA-co-AGluOH)s displayed similar thermal stabilities (T_{d5} = 268–273 °C), regardless of the molecular weights. A substantial difference was observed in the T_g values. For instance, the T_g values of P(nBA-co-AGluOH)s synthesized by RAFT copolymerization decrease slightly from 0.8 to −6.0 °C with increasing the molecular weights. This tendency may be due to the higher content of the end-groups and the absence of low-molecular-weight products, which are probably removed during the purification process, resulting in lower polymer yield (*e.g.*, 60% at [nBA]/[AGluOH]/[CTA]/[AIBN] = 150/50/2/1). P(nBA-co-AGluOH)s prepared by free radical copolymerization exhibited similar molecular weight-dependent tendency, demonstrating the higher T_g value (16.5 °C for M_n = 18 300) and lower one (−17.5 °C for M_n = 21 500). RAFT-synthesized P(nBA-co-AGluOH) with relatively high molecular weights (M_n = 14 700 and 15 900) was obtained as a rubbery sample with good stability and film-forming ability. Low-molecular-weight P(nBA-co-AGluOH) (M_n = 9500) afforded a sample, but its mechanical properties were relatively poor (Fig. 6e). The RAFT-synthesized P(nBA-co-AGluOH)s (nBA content = approximately 80 mol%) with different molecular weights demonstrated moderate Young's moduli in the range of 5.0–92 MPa. The strain of the RAFT-synthesized P(nBA-co-AGluOH)s increased with increasing molecular weight. The same tendency, where higher molecular weight led to higher strain, was also observed for P(nBA-co-AGluOH) prepared by free radical copolymerization. A substantial increase in the modulus of toughness was observed for P(nBA-co-AGluOH)s designed by RAFT and free-radical copolymerization. Interestingly, P(nBA-co-AGluOH) having the highest molecular weight (M_n = 21 500, M_w/M_n = 2.73), exhibited relatively high tensile strength (4.8 MPa) and modulus of toughness (22.28 MJ m^{-3}), yet possessed a strain at break of 634%. In contrast, P(nBA-co-AGluOH) having lowest molecular-weight (M_n = 7800), which was prepared using a dithiocarbamate-type CTA, afforded viscous product with fluid property, even if almost the same nBA content (82%, Table S10 and Fig. S16†). These results imply that the molecular weight has a remarkable effect on the mechanical properties, particularly the flexibility and toughness.

Optical properties

In addition to the mechanical and self-healing properties, integration with additional functions is desirable for future applications of self-healable materials (*e.g.*, soft robotics, sensors, electronic devices).[74,75] Here, we focused on achieving good optical properties, including transparency and improved refractive index, because the simultaneous achievement of a high refractive index with good mechanical and self-healing properties remains a challenge. Based on the Lorentz–Lorenz equation, molar refraction and molecular volume are crucial parameters to determine refractive index.[76] Hydrogen bonds have been recently employed to increase the refractive index *via* decreasing the free volume.[77] Here, P(nBA-co-AGluOH)s having different AGluOH contents (49–8 mol%) were employed to achieve good transparency and high refractive indexes *via* tuning intermolecular hydrogen bonds. As illustrated in Fig. 7, P(nBA-co-AGluOH)s demonstrated good film-
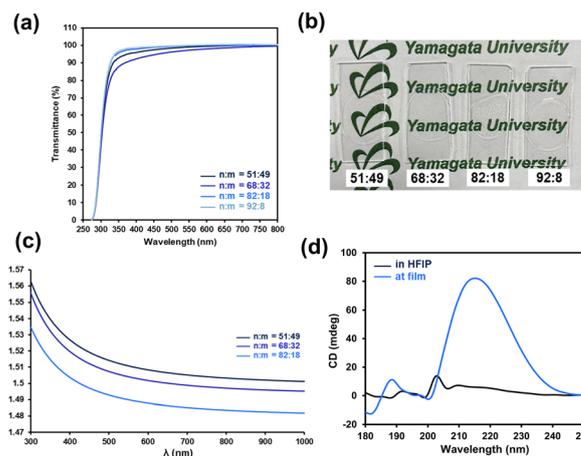

Fig. 7 (a) UV–vis transmittance spectra of P(nBA-co-AGluOH)s having different AGluOH contents (49–8 mol%) and (b) photographs of P(nBA-co-AGluOH)s films utilized for transmittance measurements, (c) wavelength-dependent refractive indices determined by ellipsometry, and (d) CD spectra of P(nBA-co-AGluOH) in HFIP (0.03 g L^{-1}) and at the film state on a quartz plate.

forming properties and good transparency in the visible region (>90% at 400 nm), regardless of the comonomer composition. The ellipsometry measurements of P(nBA-co-AGluOH)s indicated typical wavelength-dependent refractive indices (Fig. 7c), which increased from 1.4883 to 1.5089 with decreasing Abbe numbers from 63.5–56.7 by increasing AGluOH content (Table S11†). These values are comparable to those of poly(methyl methacrylate) (refractive index = 1.49 and Abbe number = 58),[78] and silicon and acrylic intraocular lenses (refractive index = 1.41–1.55 and Abbe number = 37–58).[79] These results implied that the AGluOH having hydrogen bonding ability can efficiently enhance the refractive index, while maintaining good transparency.

Chiroptical properties of P(nBA-co-AGluOH) in solid and solution states were evaluated by circular dichroism (CD) measurement. As shown in Fig. 7d, a positive CD peak at approximately 215 nm appeared in the film state, whereas no remarkable peak was detected in the hexafluoroisopropanol (HFIP) solution, showing aggregation-induced CD effect. The P(nBA-co-AGluOH)s exhibited good transparency, tunable refractive index, aggregation-induced CD effect, in addition to tunable flexibility and self-healing properties. This approach provides a practical and efficient method for the preparation of self-healable polymers with tunable properties by simple radical copolymerization of amino acid-carrying monomers, which can open new avenues for advanced optical materials, such as ophthalmic optics.

Conclusion

In summary, we developed a series of amino acid-bearing acrylamide/nBA copolymers with good mechanical and self-healing properties under ambient conditions by selecting suitable amino acid units, comonomer compositions, and molecular weights. Combining noncovalent interactions (*e.g.*, hydrogen bonds, electrostatic interactions, and π–π stacking) from the amino acid motifs and flexibility from nBA can be

achieved by copolymerizing charged monomers with a neutral monomer under suitable conditions. The nature of the amino acids (AThrOH, AGluOH, APheOH, and APhePheOH) and amino acid-bearing acrylamide/nBA content substantially affected the thermal, mechanical, and self-healing properties. The molecular weight of the copolymers is also a crucial factor for manipulating the mechanical strength. The AGluOH content in P(nBA-co-AGluOH) efficiently enhanced the refractive indices while maintaining good transparency by tuning the noncovalent interactions. This strategy is regarded as physical and reversible crosslinking *via* noncovalent interactions derived from naturally originating amino acid motifs, which can contribute to the tuning of thermal, mechanical, and self-healing properties, as well as optical properties involving transparency and refractive index.

Data availability

The data that support the findings of this study are available from the corresponding author upon reasonable request.

Author contributions

Ryo Kudo: investigation, methodology, writing – original draft. Sadaki Samitsu: investigation, validation, writing – review & editing. Hideharu Mori: conceptualization, supervision, validation, writing – review & editing.

Conflicts of interest

There are no conflicts to declare.

Acknowledgements

Notes and references

1 A. Campanella, D. Dohler and W. H. Binder, *Macromol. Rapid Commun.*, 2018, **39**, e1700739.

2 C. Kim and N. Yoshie, *Polym. J.*, 2018, **50**, 919–929.

3 Y. Yang and M. W. Urban, *Adv. Mater. Interfaces*, 2018, **5**, 1800384.

4 C. E. Diesendruck, N. R. Sottos, J. S. Moore and S. R. White, *Angew. Chem., Int. Ed.*, 2015, **54**, 10428–10447.

5 S. R. White, N. R. Sottos, P. H. Geubelle, J. S. Moore, M. R. Kessler, S. R. Sriram, E. N. Brown and S. Viswanathan, *Nature*, 2001, **409**, 794–797.

6 M. Gragert, M. Schunack and W. H. Binder, *Macromol. Rapid Commun.*, 2011, **32**, 419–425.

7 H. Ying, Y. Zhang and J. Cheng, *Nat. Commun.*, 2014, **5**, 3218.

8 Z. Wang, S. Gangarapu, J. Escorihuela, G. Fei, H. Zuilhof and H. Xia, *J. Mater. Chem. A*, 2019, **7**, 15933–15943.

9 Y. Amamoto, J. Kamada, H. Otsuka, A. Takahara and K. Matyjaszewski, *Angew Chem. Int. Ed. Engl.*, 2011, **50**, 1660–1663.

10 J. Canadell, H. Goossens and B. Klumperman, *Macromolecules*, 2011, **44**, 2536–2541.

11 U. Lafont, H. van Zeijl and S. van der Zwaag, *ACS Appl. Mater. Interfaces*, 2012, **4**, 6280–6288.

12 J. Bai, H. Li, Z. Shi and J. Yin, *Macromolecules*, 2015, **48**, 3539–3546.

13 J. Kötteritzsch, S. Stumpf, S. Hoeppener, J. Vitz, M. D. Hager and U. S. Schubert, *Macromol. Chem. Phys.*, 2013, **214**, 1636–1649.

14 K. K. Oehlenschlaeger, J. O. Mueller, J. Brandt, S. Hilf, A. Lederer, M. Wilhelm, R. Graf, M. L. Coote, F. G. Schmidt and C. Barner-Kowollik, *Adv. Mater.*, 2014, **26**, 3561–3566.

15 T. Liu, C. Hao, S. Zhang, X. Yang, L. Wang, J. Han, Y. Li, J. Xin and J. Zhang, *Macromolecules*, 2018, **51**, 5577–5585.

16 J. Tan, C. Li, K. De Bruycker, G. Zhang, J. Gu and Q. Zhang, *RSC Adv.*, 2017, **7**, 51763–51772.

17 P. Cordier, F. Tournilhac, C. Soulie-Ziakovic and L. Leibler, *Nature*, 2008, **451**, 977–980.

18 D. Montarnal, P. Cordier, C. Soulié-Ziakovic, F. Tournilhac and L. Leibler, *J. Polym. Sci., Part A: Polym. Chem.*, 2008, **46**, 7925–7936.

19 D. Montarnal, F. Tournilhac, M. Hidalgo, J. L. Couturier and L. Leibler, *J. Am. Chem. Soc.*, 2009, **131**, 7966–7967.

20 T. L. Sun, T. Kurokawa, S. Kuroda, A. Bin Ihsan, T. Akasaki, K. Sato, M. A. Haque, T. Nakajima and J. P. Gong, *Nat. Mater.*, 2013, **12**, 932–937.

21 S. Burattini, B. W. Greenland, D. H. Merino, W. Weng, J. Seppala, H. M. Colquhoun, W. Hayes, M. E. Mackay, I. W. Hamley and S. J. Rowan, *J. Am. Chem. Soc.*, 2010, **132**, 12051–12058.

22 J. Fox, J. J. Wie, B. W. Greenland, S. Burattini, W. Hayes, H. M. Colquhoun, M. E. Mackay and S. J. Rowan, *J. Am. Chem. Soc.*, 2012, **134**, 5362–5368.

23 L. R. Hart, J. H. Hunter, N. A. Nguyen, J. L. Harries, B. W. Greenland, M. E. Mackay, H. M. Colquhoun and W. Hayes, *Polym. Chem.*, 2014, **5**, 3680–3688.

24 S. Bode, L. Zedler, F. H. Schacher, B. Dietzek, M. Schmitt, J. Popp, M. D. Hager and U. S. Schubert, *Adv. Mater.*, 2013, **25**, 1634–1638.

25 W. Weng, J. B. Beck, A. M. Jamieson and S. J. Rowan, *J. Am. Chem. Soc.*, 2006, **128**, 11663–11672.

26 Y. Zhao, J. B. Beck, S. J. Rowan and A. M. Jamieson, *Macromolecules*, 2004, **37**, 3529–3531.

27 B. Guo, Y. Liang and R. Dong, *Nat. Protoc.*, 2023, **18**, 3322–3354.

28 S. Zhuo, Y. Liang, Z. Wu, X. Zhao, Y. Han and B. Guo, *Mater. Horiz.*, 2024, **11**, 37–101.

29 L. Cai, S. Liu, J. Guo and Y.-G. Jia, *Acta Biomater.*, 2020, **113**, 84–100.

30 S. Sharma, A. Kumar, Deepak, R. Kumar, N. K. Rana and B. Koch, *Int. J. Biol. Macromol.*, 2018, **116**, 37–44.

31 H. An, L. Zhu, J. Shen, W. Li, Y. Wang and J. Qin, *Colloids Surf., B*, 2020, **185**, 110601.

32 S. Dai, X. Zhou, S. Wang, J. Ding and N. Yuan, *Nanoscale*, 2018, **10**, 19360–19366.

33 R. Yang, X. Liu, Y. Ren, W. Xue, S. Liu, P. Wang, M. Zhao, H. Xu and B. Chi, *Acta Biomater.*, 2021, **127**, 102–115.

34 Q. Wang, Z. Shi, Y. Shou, K. Zhang, G. Li, P. Xia, S. Yan and J. Yin, *ACS Biomater. Sci. Eng.*, 2020, **6**, 1715–1726.

35 A. Phadke, C. Zhang, B. Arman, C.-C. Hsu, R. A. Mashelkar, A. K. Lele, M. J. Tauber, G. Arya and S. Varghese, *Proc. Natl. Acad. Sci. U. S. A.*, 2012, **109**, 4383–4388.

36 X. Dai, Y. Zhang, L. Gao, T. Bai, W. Wang, Y. Cui and W. Liu, *Adv. Mater.*, 2015, **27**, 3566–3571.

37 S.-n. Nishimura, D. Sato and T. Koga, *Gels*, 2023, **9**, 829.

38 T. Koga, K. Tomimori and N. Higashi, *Macromol. Rapid Commun.*, 2020, **41**, 1900650.

39 M. Hendrich, L. Lewerdomski and P. Vana, *J. Polym. Sci., Part A: Polym. Chem.*, 2015, **53**, 2809–2819.

40 T. Koga, T. Morishita, Y. Harumoto, S.-n. Nishimura and N. Higashi, *Mater. Adv.*, 2021, **2**, 7851–7860.

41 S. Tazawa, A. Shimojima, T. Maeda and A. Hotta, *J. Appl. Polym. Sci.*, 2018, **135**, 45419.

42 D. Zaguri, S. Shaham-Niv, P. Chakraborty, Z. Arnon, P. Makam, S. Bera, S. Rencus-Lazar, P. R. Stoddart, E. Gazit and N. P. Reynolds, *ACS Appl. Mater. Interfaces*, 2020, **12**, 21992–22001.

43 K. Baek, A. D. Noblett, P. Ren and L. J. Suggs, *ACS Appl. Bio Mater.*, 2019, **2**, 2812–2821.

44 N. Zanna, A. Merlettini and C. Tomasini, *Org. Chem. Front.*, 2016, **3**, 1699–1704.

45 W. Wang, Z. Liu, Z. Guo, J. Zhang, C. Li, S. Qiu, X. Lei and Q. Zhang, *ACS Appl. Mater. Interfaces*, 2020, **12**, 50812–50822.

46 R. K. Bose, N. Hohlbein, S. J. Garcia, A. M. Schmidt and S. van der Zwaag, *Phys. Chem. Chem. Phys.*, 2015, **17**, 1697–1704.

47 Y. Hou, Y. Peng, P. Li, Q. Wu, J. Zhang, W. Li, G. Zhou and J. Wu, *ACS Appl. Mater. Interfaces*, 2022, **14**, 35097–35104.

48 J. Li, H. Ejima and N. Yoshie, *ACS Appl. Mater. Interfaces*, 2016, **8**, 19047–19053.

49 C. Kim, H. Ejima and N. Yoshie, *RSC Adv.*, 2017, 19288–19295.

50 L. Laysandra, C.-H. Chuang, S. Kobayashi, A.-N. Au-Duong, Y.-H. Cheng, Y.-T. Li, M. M. Mburu, T. sono, T. Satoh and Y.-C. Chiu, *ACS Appl. Polym. Mater.*, 2020, **2**, 5432–5443.

51 S. Chen, G. Ma, X. Duan, H. Zhuo, J. Xu and H. Chen, *ACS Appl. Polym. Mater.*, 2023, **5**, 6390–6398.

52 S. Wang, L. Li, Q. Liu and M. W. Urban, *Macromolecules*, 2022, **55**, 4703–4709.

53 Y. Zhou, G. Chen, S. Yan, C. Ni, L. Yu and X. Li, *Prog. Org. Coat.*, 2022, **172**, 107098.

54 W. Wang, F. Wang, C. Zhang, J. Tang, X. Zeng and X. Wan, *Chem. Eng. J.*, 2021, **404**, 126358.

55 S. Wang and M. W. Urban, *Adv. Sci.*, 2021, **8**, 2101399.

56 S. S. Halacheva, D. J. Adlam, E. K. Hendow, T. J. Freemont, J. Hoyland and B. R. Saunders, *Biomacromolecules*, 2014, **15**, 1814–1827.

57 D. Cao, Y. Zhang, Z. Cui, Y. Du and Z. Shi, *Mater. Sci. Eng., C*, 2017, **70**, 665–672.

58 M. Prasitsilp, T. Siriwittayakorn, R. Molloy, N. Suebsanit, P. Siriwittayakorn and S. Veeranondha, *J. Mater. Sci.: Mater. Med.*, 2003, **14**, 595–600.

59 C. A. Schoener, H. N. Hutson and N. A. Peppas, *AIChE J.*, 2013, **59**, 1472–1478.

60 A. Mayer, T. Roch, K. Kratz, A. Lendlein and F. Jung, *Acta Biomater.*, 2012, **8**, 4253–4259.

61 G. Rodriguez, M. Fernandez-Gutierrez, J. Parra, A. Lopez-Bravo, N. G. Honduvilla, J. Bujan, M. Molina, L. Duocastella and J. San Roman, *Biomacromolecules*, 2010, **11**, 2740–2747.

62 J. Cui, K. Trescher, K. Kratz, F. Jung, B. Hiebl and A. Lendlein, *Clin. Hemorheol. Microcirc.*, 2010, **45**, 401–411.

63 K. Shoji, M. Nakayama, T. Koseki, K. Nakabayashi and H. Mori, *Polymer*, 2016, **97**, 20–30.

64 M. P. Bueno, C. A. Cativiela, J. A. Mayoral and A. Avenoza, *J. Org. Chem.*, 1991, **56**, 6551–6555.

65 T. Koseki, R. Kanto, R. Yonenuma, K. Nakabayashi, H. Furusawa, S. Yano and H. Mori, *React. Funct. Polym.*, 2020, **150**, 104540.

66 S. Y. Park, S.-Y. Kim, T. Kim, H. Ahn and I. Chung, *Polym. Adv. Technol.*, 2019, **30**, 872–878.

67 H. Mori, M. Matsuyama, K. Sutoh and T. Endo, *Macromolecules*, 2006, **39**, 4351–4360.

68 R. Yonenuma, A. Ishizuki, K. Nakabayashi and H. Mori, *J. Polym. Sci., Part A: Polym. Chem.*, 2019, **57**, 2562–2574.

69 J. Liu, H. Su, L. Meng, Y. Zhao, C. Deng, J. C. Y. Ng, P. Lu, M. Faisal, J. W. Y. Lam, X. Huang, K. S. Wong and B. Z. Tang, *Chem. Sci.*, 2012, **3**, 2737–2747.

70 H. Tanaka, Y. Inoue and T. Mori, *ChemPhotoChem*, 2018, **2**, 386–402.

71 Y. Sang, J. Han, T. Zhao, P. Duan and M. Liu, *Adv. Mater.*, 2020, **32**, 1900110.

72 G. Dado and S. Gellman, *J. Am. Chem. Soc.*, 1994, **116**, 1054–1062.

73 K. Tsang, H. Diaz, N. Graciani and J. Kelly, *J. Am. Chem. Soc.*, 1994, **116**, 3988–4005.

74 W. Zhang, H. Jiang, Z. Chang, W. Wu, G. WWu, R. Wu and J. Li, *J. Mater. Sci.*, 2020, **55**, 13543–13558.

75 Y. J. Tan, G. J. Susanto, H. P. Anwar Ali and B. C. K. Tee, *Adv. Mater.*, 2021, **33**, 2002800.

76 J.-g. Liu and M. Ueda, *J. Mater. Chem.*, 2009, **19**, 8907–8919.

77 S. Watanabe, H. Nishio, T. Takayama and K. Oyaizu, *ACS Appl. Polym. Mater.*, 2023, **5**, 2307–2311.

78 G. S. Jha, G. Seshadri, A. Mohan and R. K. Khandal, *e-Polymers*, 2007, 120.

79 M. Vacalebre, R. Frison, C. Corsaro, F. Neri, A. Santoro, S. Conoci, E. Anastasi, M. C. Curatolo and E. Fazio, *Polymers*, 2023, **15**, 1590.